Supplement of The Cryosphere, 12, 2883–2900, 2018
https://doi.org/10.5194/tc-12-2883-2018-supplement

The Cryosphere Open Access EGU

Supplement of

Mechanisms leading to the 2016 giant twin glacier collapses, Aru Range, Tibet

Adrien Gilbert et al.

Correspondence to: Adrien Gilbert (adrien@geo.uio.no)

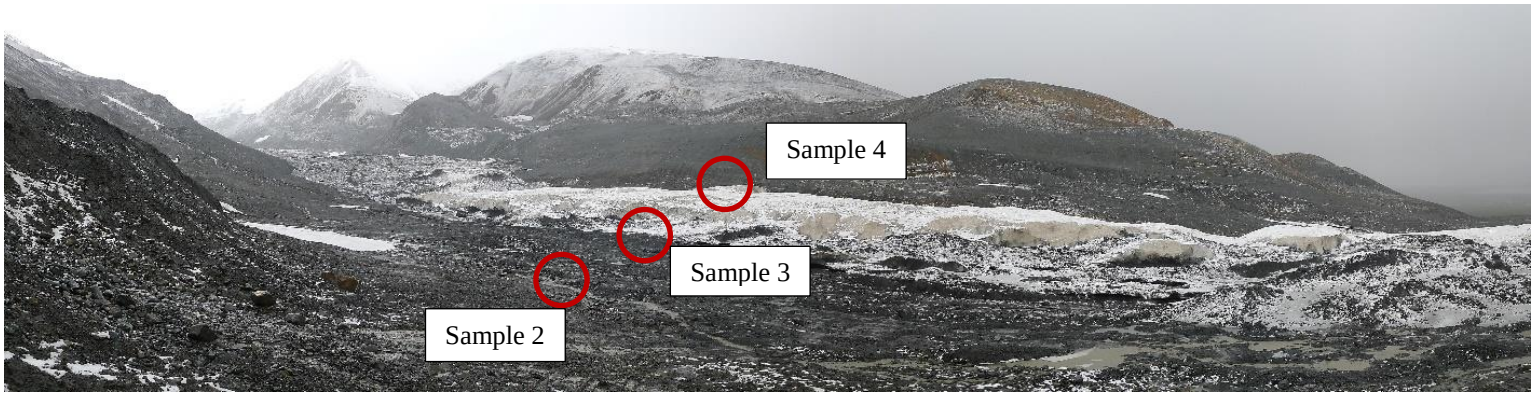

Figure S1 – Overview of the sampling area in the gorge close to the former glacier terminus of Aru-1 glacier. The picture was taken during a July 2017 field trip and shows the soft and erodible lithology on which Aru glaciers flowed. See also Figure 12 of the manuscript.

Figure S2 – Small gorge where sample 1 has been collected. See also Figure 12 of the manuscript.

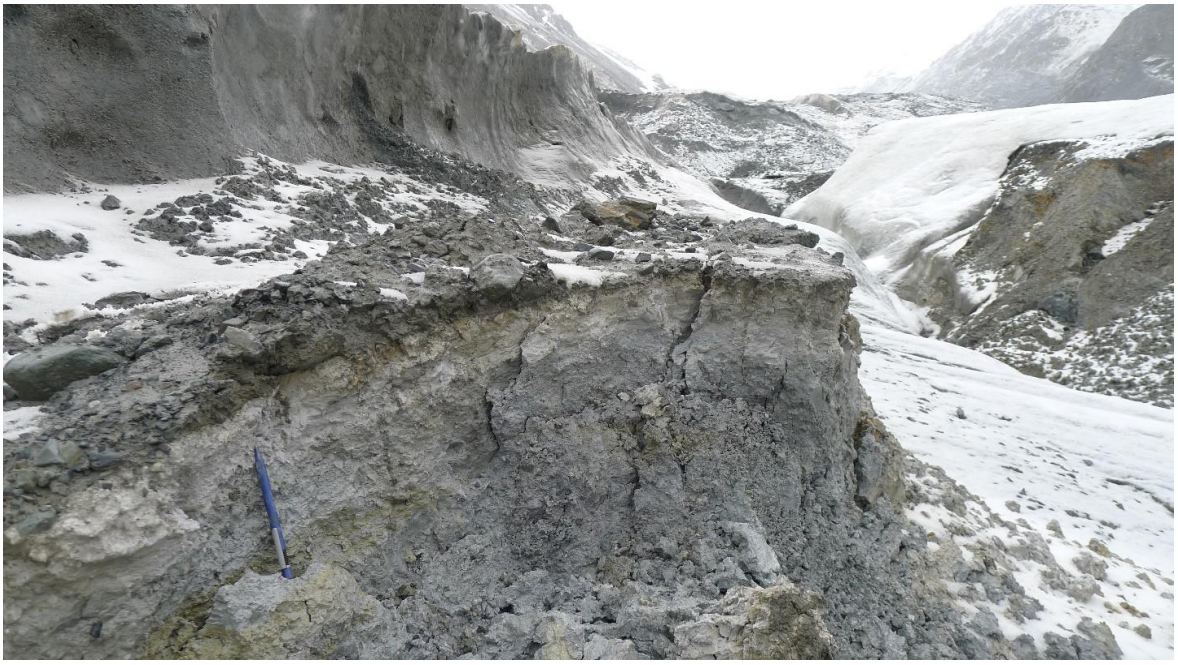

Figure S3 – Clay bellow collapse deposit. Sample no 4.

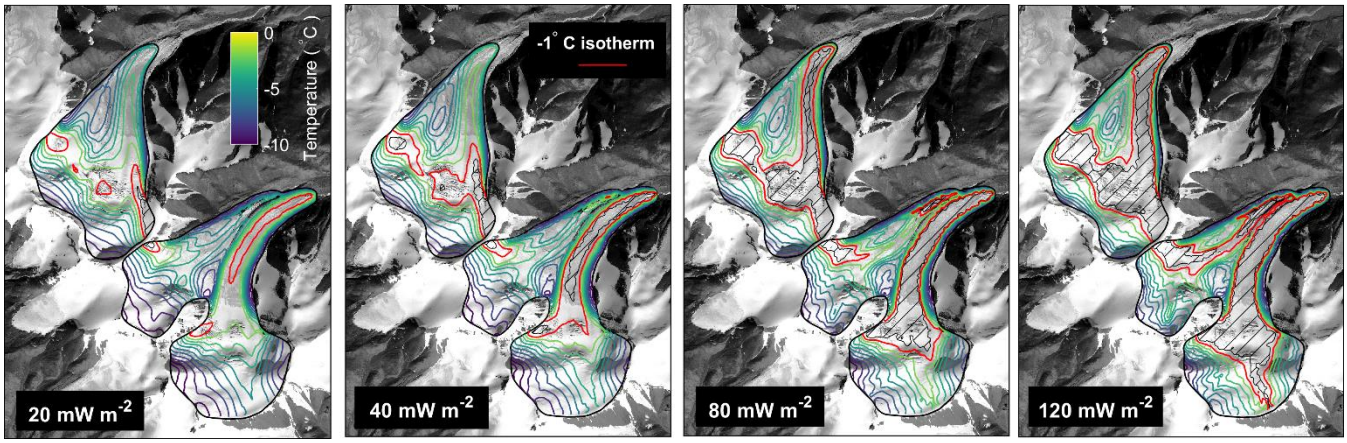

Figure S4 – Steady state temperature at the glacier base modeled for different values of basal heat flux. The results presented in the manuscript assume 80 mW m^{-2}.

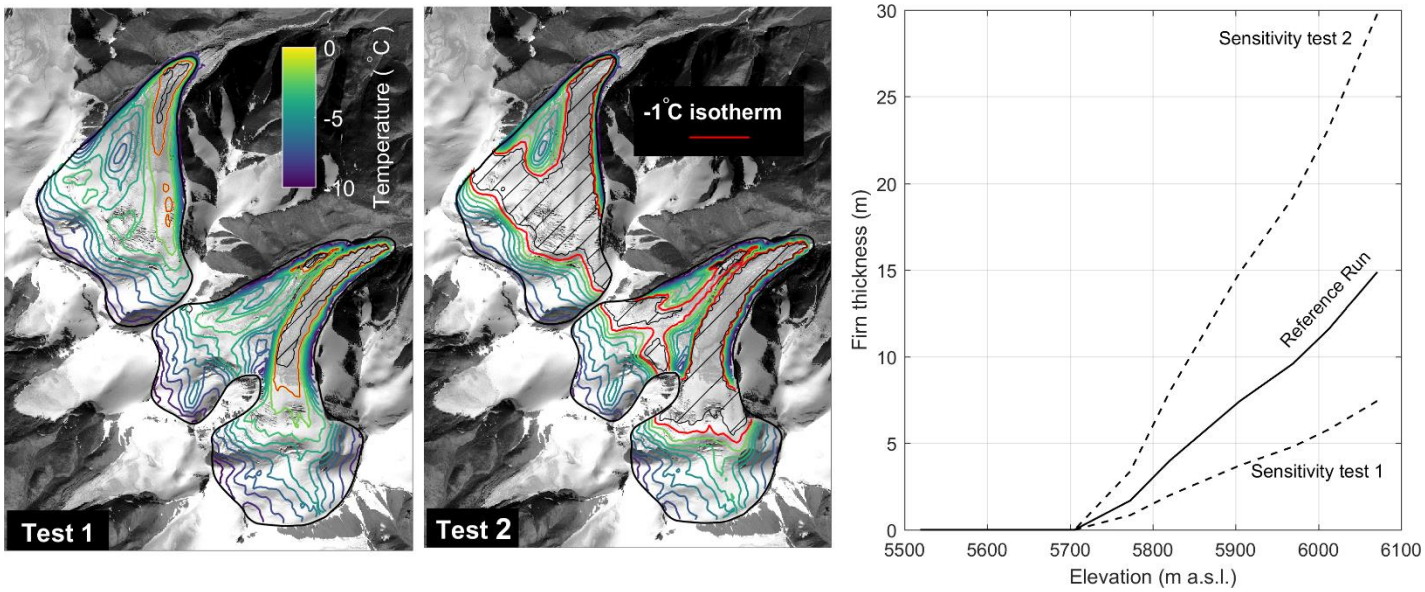

Figure S5 – Steady state temperature modelled at the glacier base modeled for two different firn thickness hypothesis (1) and (2). This two hypothesis are plotted on the right figure and compared with the firn thickness assumed in the manuscript (reference run).

5

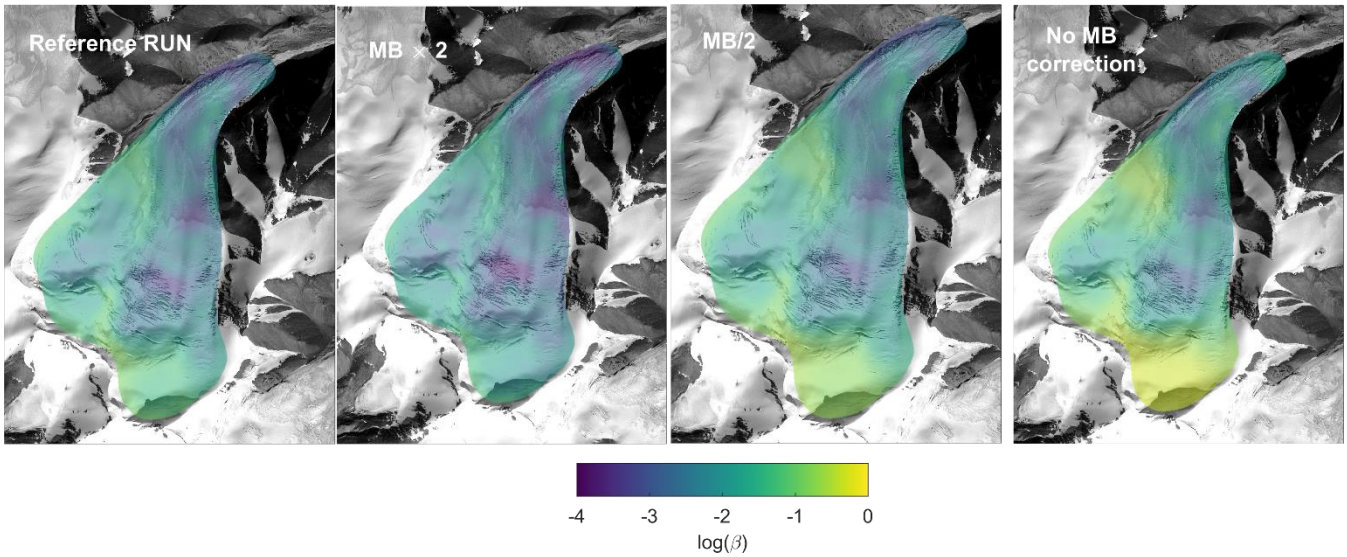

Figure S6 - Friction coefficient β inferred for different surface mass balance modifications on Aru-1 glacier between 2013 and 2014: (i) modeled surface mass balance multiplied by 2, (ii) modeled surface mass balance divided by two and (iii) no surface mass balance correction. The friction field variability presented here is a conservative estimate of the uncertainty introduced by the surface mass balance. It shows that friction in the detachment area where surface-normal velocities are high, due to unbalanced geometry, are not very sensitive to surface mass balance reconstruction. This makes our results reliable in this part of the glacier, which is the focus of the study.

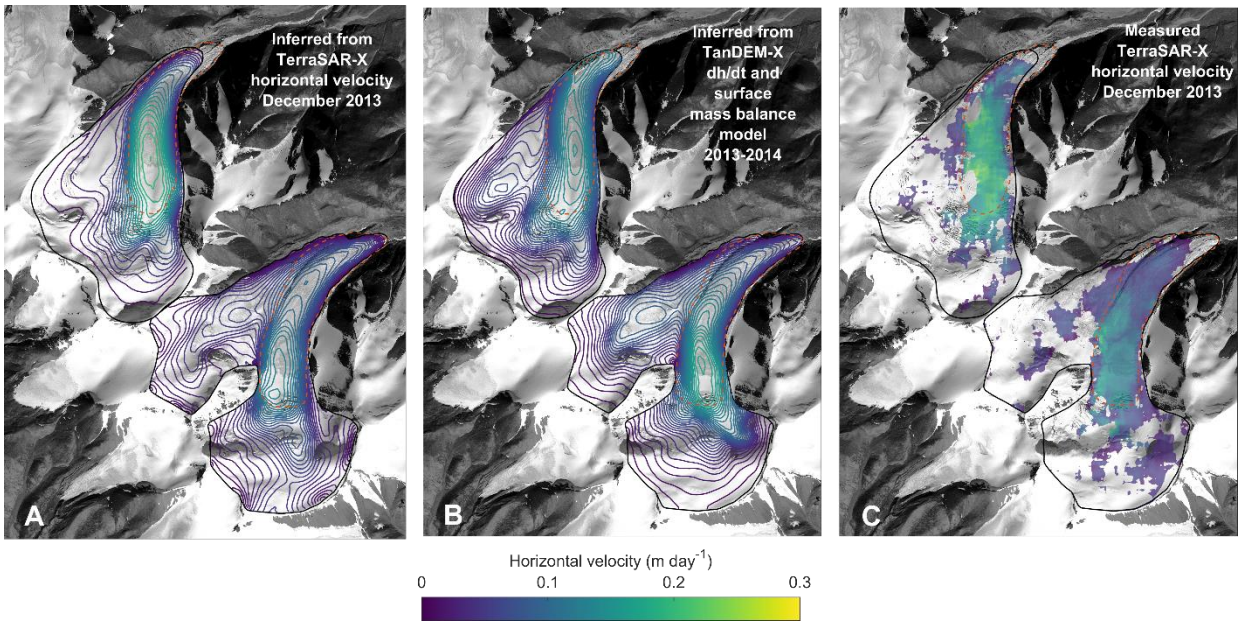

Figure S7 - Surface horizontal velocity modeled with basal friction coefficient inferred from horizontal velocity measurement (A) and from emergence velocity estimation (B). (C) Measured horizontal velocity between 2013-11-30 and 2013-12-11 from TerraSAR-X offset tracking.

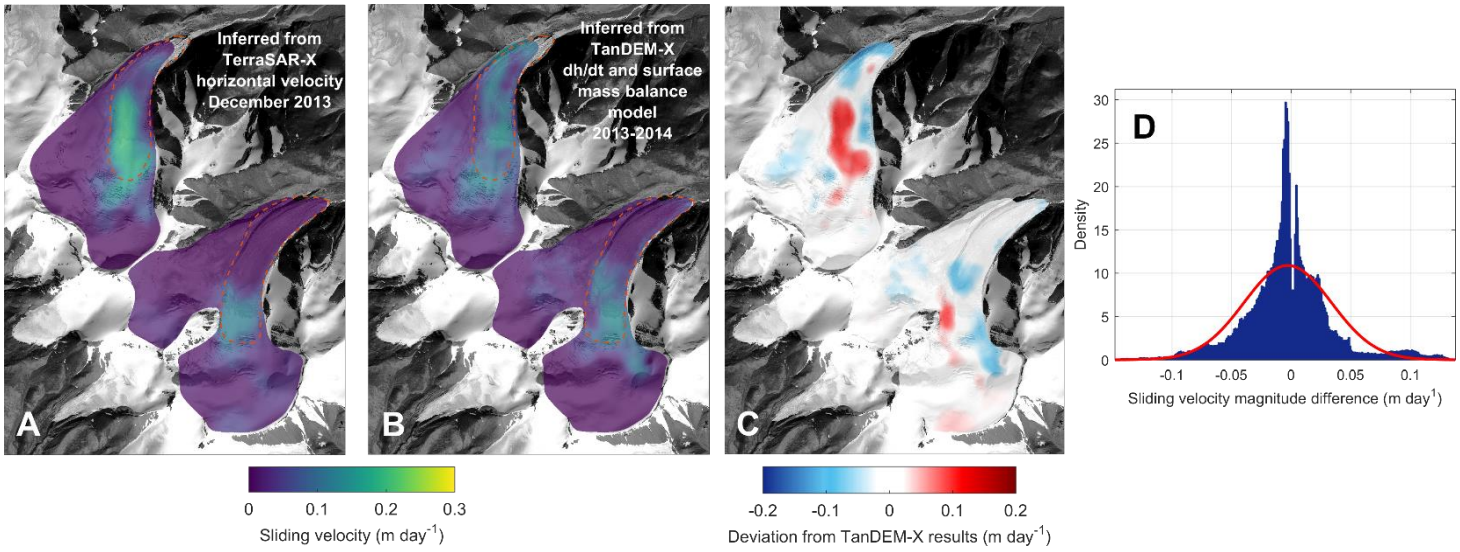

Figure S8 - Sliding horizontal velocity modeled with basal friction coefficient inferred from horizontal velocity measurement (A) and from emergence velocity estimation (B). (C) shows difference between (A) and (B) and (D) is the associated error distribution (blue) and Gaussian fit (red).

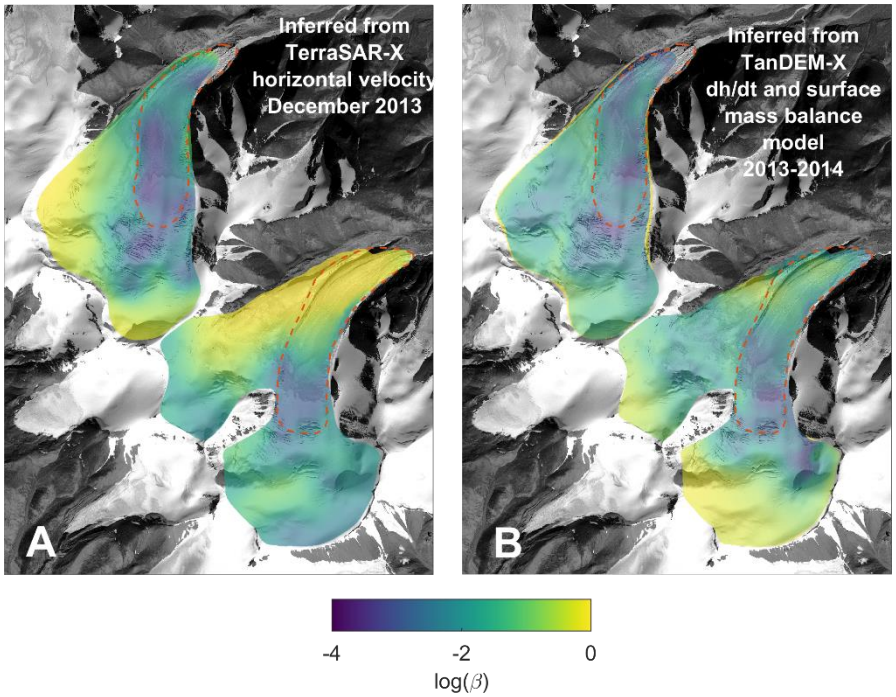

Figure S9 - Basal friction coefficient β inferred from horizontal velocity measurement (A) and from emergence velocity estimation (B).

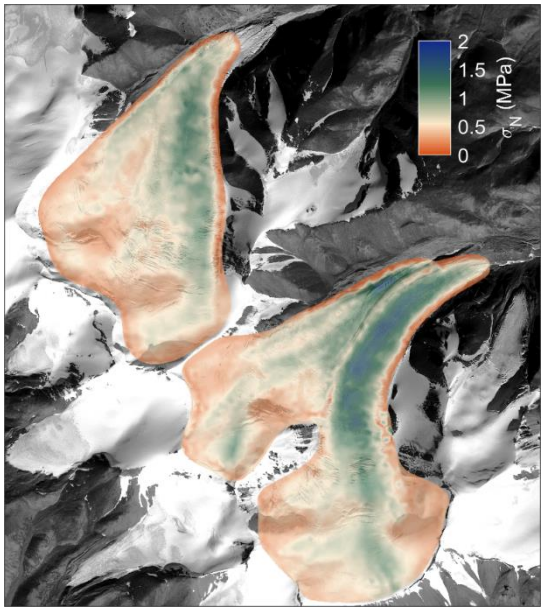

Figure S10 – Modeled basal normal stress for steady state geometry